Low Power Reflective Display with Print-Like Color via Novel Electronic Inks

Zhang-Lin Zhou, Jong-Souk Yeo, Qin Liu, Mary Parent, June Yang, Brad Benson, Greg Combs, Jeff Mabeck, Sity Lam, Yoocharn Jeon, Dick Henze, Tim Koch

HP Laboratories
HPL-2011-67

Keyword(s):

Reflective display, Print-like color, Electrokinetic technology, Electronic inks, Roil-to-Roll manufacturing

Abstract:

Reflective display technologies aim to enable the delivery of dynamic digital content to devices that have the look and feel of ink on paper. We are presenting herein a novel device architecture design and proprietary electrically addressable inks, which enable low power, disruptive, print-like full color reflective display that can exceed the chromaticity represented by the Specifications for Newsprint Advertising Production (SNAP) standard. We are approaching the challenge of generating bright high-quality reflective color images from the perspective of printing by stacking electro-optic layers of subtractive colorants to address every available color at every location. Using in-plane optical effects, our novel media technology provides fast switching between clear and color states. Thin, flexible electronic media based on this technology has been fabricated by imprinting three-dimensional micro-scale structures with a continuous roll-to-roll (R2R) manufacturing platform. HP's combination of novel device architecture, proprietary inks, and R2R manufacturing platform enables the required attributes for electronic media such as flexibility, robustness, low power, transparency, print-quality color, and scalability at low cost. The structure property relationship of surfactants has been carried out; their impact on performance of display devices has been studied. These results have been applied to improve the performance of electronic inks. We have demonstrated 3-layer stacked segmented reflective display prototypes, as well as pixelated stacked color reflective display prototypes. The innovations described in this paper are applicable to electronic skins for customizable electronic surfaces and are currently being developed further for electronic paper and signage markets.

External Posting Date: May 21, 2011 [Fulltext] Approved for External Publication
Internal Posting Date: May 21, 2011 [Fulltext]

Low Power Reflective Display with Print-Like Color via Novel Electronic Inks

Zhang-Lin Zhou[1], Jong-Souk Yeo[2,3], Qin Liu[2], Mary Parent[1], June Yang[1], Brad Benson[2], Greg Combs[2], Jeff Mabeck[2], Sity Lam[1], Yoocharn Jeon[1], Dick Henze[1], Tim Koch[2]

[1] Next Generation Display, Mobile and Immersive Experience Lab, Hewlett Packard Labs, Hewlett-Packard Company, 1501 Page Mill Road, Palo Alto 94304, CA 94304, USA

[2] Flexible Information Service Technology (FIST), Hewlett-Packard Company, 1000 NE Circle Blvd., Corvallis, Oregon, USA

[3] Current address: School of Integrated Technology, Yonsei University, 162-1 Songdo-dong, Yeonsu-gu, Incheon, Korea

ABSTRACT

Reflective display technologies aim to enable the delivery of dynamic digital content to devices that have the look and feel of ink on paper. We are presenting herein a novel device architecture design and proprietary electrically addressable inks, which enable low power, disruptive, print-like full color reflective display that can exceed the chromaticity represented by the Specifications for Newsprint Advertising Production (SNAP) standard. We are approaching the challenge of generating bright high-quality reflective color images from the perspective of printing by stacking electro-optic layers of subtractive colorants to address every available color at every location. Using in-plane optical effects, our novel media technology provides fast switching between clear and color states. Thin, flexible electronic media based on this technology has been fabricated by imprinting three-dimensional micro-scale structures with a continuous roll-to-roll (R2R) manufacturing platform. HP's combination of novel device architecture, proprietary inks, and R2R manufacturing platform enables the required attributes for electronic media such as flexibility, robustness, low power, transparency, print-quality color, and scalability at low cost. The structure property relationship of surfactants has been carried out; their impact on performance of display devices has been studied. These results have been applied to improve the performance of electronic inks. We have demonstrated 3-layer stacked segmented reflective display prototypes, as well as pixelated stacked color reflective display prototypes. The innovations described in this paper are applicable to electronic skins for customizable electronic surfaces and are currently being developed further for electronic paper and signage markets.

INTRODUCTION

Reflective displays have seen tremendous growth recently with their application to eBook readers, enabled by the widespread adoption of E Ink Corporation's micro-encapsulated black and white electrophoretic display film [1]. This growth continues to drive technology development in related frontplane and backplane technologies, and especially in their integration required to provide compelling color solutions [2]. Conventional displays typically use a

combination of side-by-side color elements to generate additive color (*e.g.*, RGB or RGBW color filters), and this approach has been shown by others with black and white reflective electro-optic layers. Since reflective images rely solely on ambient light, the image will be bright and colorful only if the incident light is reflected efficiently. Side-by-side color approaches devote portions of each pixel to only certain colors, so they inherently absorb the majority of the incident light, and thus are inefficient (<50% efficiency), resulting in limited color gamut volume [2].

At Hewlett-Packard (HP), we are approaching the challenge of generating bright, high-quality reflective color images from the perspective of printing by layering subtractive colorants (CMYK) to allow every available color at every addressable pixel location. Layered colorants in electronic media can be enabled by stacking electro-optic layers that are modulated between colored and transparent optical states. In order to provide a transparent state with fast switching using circuits fabricated on a plastic substrate by a flexible roll-to-roll (R2R) manufacturing platform, HP has developed a novel electrokinetic frontplane architecture with electrically addressable inks. We have previously reported the application of HP's electrokinetic media to thin, flexible, segmented, and reflective "electronic skins" (eSkins) [3,4].

Capability to integrate this novel reflective color media with active matrix backplanes is the key to enabling pixelated reflective displays beyond eSkins. In order to provide full color with stacked architecture of layered colorants, each colorant layer needs to be addressed with electrical interconnect, either by providing vias from a common electronics layer, or by integration of a suitably transparent matrix of driving electronics. HP is developing a suitable active matrix backplane technology based on transparent oxide TFTs that are compatible with existing glass (AMLCD) fabs as well as eventual migration to a R2R manufacturing process [6].

In this paper, we report further details on our novel flexible reflective color media based on an electrokinetic technology platform and R2R manufacturing platform. We also report the structure property relationship of surfactants and their impact on ink performances. We also demonstrate further advancements in the technology by integrating the frontplane with a transparent metal oxide TFT backplane to demonstrate a pixelated active matrix reflective display.

RESULTS AND DISCUSSION

Approach to Color

For reflective color devices, printing standards (designed for reflective images) are preferable to conventional display standards (designed for emissive/transmissive images) for evaluating image quality. In the printing industry, advertisers are accustomed to standards such as the Specifications for Newsprint Advertising Production (SNAP) used for newspaper ad inserts and the Specifications for Web Offset Publications (SWOP) used for magazines and other high quality printing. Significantly, SNAP requires ~57% peak reflectivity while SWOP requires ~76% peak reflectivity, neither of which can be achieved by color filter or polarization approaches that are <50% efficient.

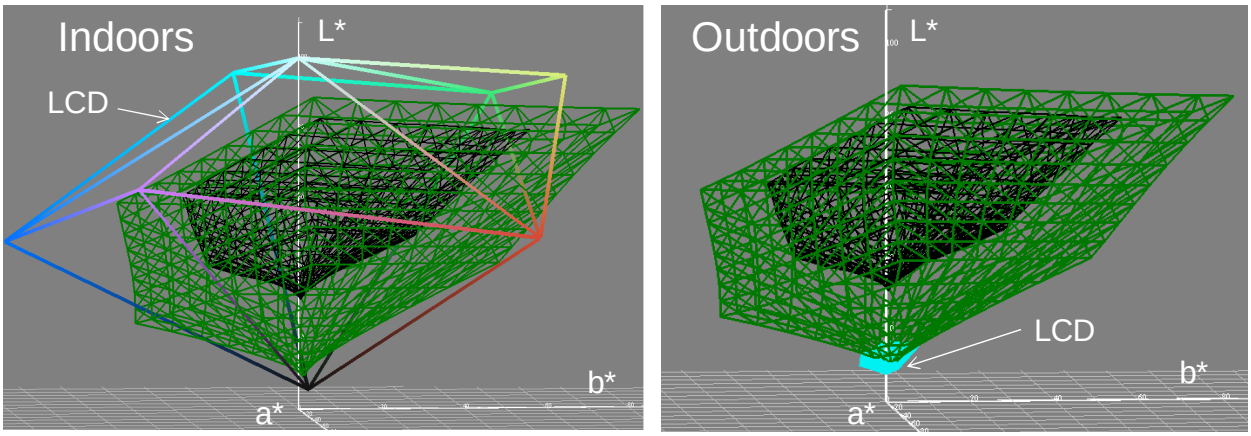

Figure 1. Color gamut volumes comparing SNAP (black interior wireframe), SWOP (green wireframe), and conventional LCD notebook display performance under typical indoor and outdoor ambient illumination.

It is also important to consider the complete color gamut achievable, not just the peak reflectivity of the white state. **Figure 1** compares the color gamut volumes of the SNAP standard, SWOP standard, and a conventional LCD notebook display, measured both in a typical indoor office environment (ambient illuminance level = 300 lux) and in a typical outdoor environment on an overcast day (ambient illuminance level = 3000 lux). You can clearly see the dramatic reduction in both the contrast and color gamut volume of the LCD display when viewed outdoors, where the gamut becomes negligible compared to print.

Figure 2 shows how brightness and contrast compare for printing and various reflective display technologies. Inkjet printing and the magazine SWOP standard have very high brightness and contrast, so they appear in the upper right-hand corner with high white state lightness values and low dark state lightness values. The HP technology presented here is predicted to exceed the SNAP printing standard using a system of layered colorants (based on optical simulations). We have demonstrated white state lightness exceeding SNAP from monochrome devices and continue to improve optical performance for full color application.

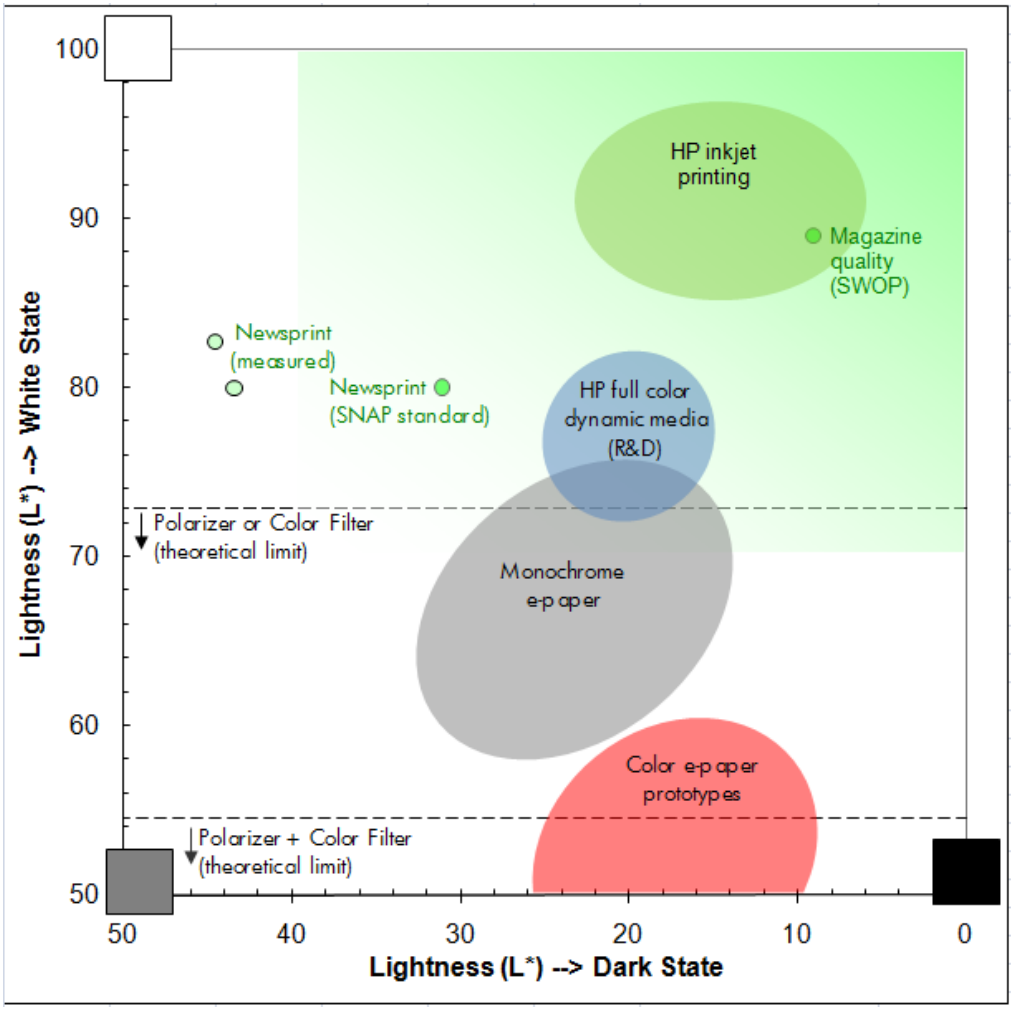

Figure 2. Brightness and contrast comparison of print and reflective display technologies. Print-like performance is in the upper right-hand quadrant (green).

Novel Reflective Frontplane

Electrokinetic Technology Platform

In order to provide a transparent state with fast switching, we have developed a novel hybrid architecture adopting out-of-plane switching fields with in-plane optical effects. In contrast, conventional electrophoretic architectures (e.g., E Ink's Pearl Imaging Film) are based on out-of-plane switching with out-of-plane optical effects, where the colorant particles are primarily moved perpendicular to the plane of the film by applying electric fields primarily perpendicular to the plane of the film [1]. These conventional architectures do not enable transparency or print-like full color. Alternative in-plane electrophoretic architectures based on in-plane switching with in-plane optical effects have been shown by IBM, Philips, and others [6][7], where the colorant particles are primarily moved parallel to the plane of the film by applying electric fields primarily parallel to the plane of the film. While the in-plane electrophoretic architectures provide a transparent state which enables stacked layers for full

color displays, they are generally limited by trade-offs between clear aperture and switching speed, and also require electrical cross-overs of in-plane electrodes, which increase the manufacturing complexity.

To address these issues, the hybrid architecture described here allows transparency in the clear state while achieving good switching speed by effectively reducing the electrode gap while maintaining a large clear aperture. Response times are improved compared to in-plane electrophoretic devices by reducing the distance the particles have to travel and increasing the driving force applied to the particles. Improved clear aperture with misalignment tolerant architecture is achieved by introducing a uniform distribution of dot arrays to minimize the areas where colorant particles are compacted. Since the control of multiple electrokinetic forces leads to the compaction of colorant particles, the technology is termed "electrokinetic" media. **Figure 3** shows schematic and microscopic images of unique colored and transparent states enabled by this architecture. Without an applied voltage, the colorant particles are spread uniformly, and the display element is in the dark state. Under a bias condition that provides compaction of colorant particles into dot-patterned cavities, the display element produces a transparent state. This transparent state can be maintained with a low-power holding voltage (<1 $\mu W/cm^2$ at ~5 V typical). We have demonstrated relatively fast switching (< 300ms) and reflectance larger than 60% (brightness L* >80) having contrast ratio of 30:1 for black and white electronic media using our proprietary black inks and white reflector background (L* ~96). Inherent advantages resulting from the control of nanoscale colorants in an out-of-plane electrode geometry are wide viewing angle (180 degrees), continuous levels of gray, and high spatial resolution (>500PPI with single dot).

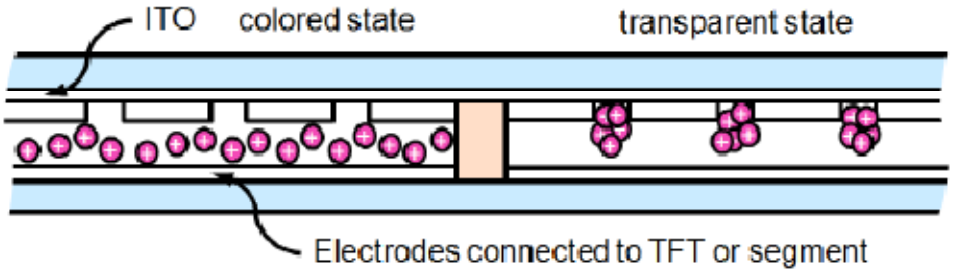

Figure 3a. Schematics of novel device architecture: Clear and dark state.

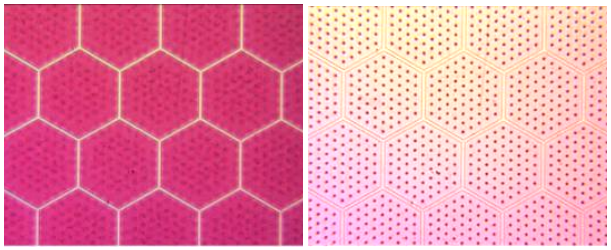

(a) Colored state (b) Transparent state

Figure 3b. Microscopic images of electrokinetic architecture.

Design and Development of Electronic Inks

A high performance electronic ink should exhibit good optical density, high mobility for fast switching speed, high cycle switching endurance, environmental stability, and low toxicity. Stable, charged colorant particle suspensions require at least the following four components: (1) colorant particle, (2) carrier fluid, (3) dispersant, and (4) charge director. The colorant particle provides the color and can participate in charging. Key considerations are the particle size, surface functional groups, dispersbility, hue, chroma, and lightness. The carrier fluid acts as a vehicle for dispersing the pigment as well as a low dielectric constant medium. When choosing the carrier fluid, its polarity, viscosity, resistivity, specific gravity, chemical stability, and toxicity must all be considered. The dispersant provides steric stabilization of the colorant particles to prevent particle aggregation. The charge director enables charging of the particles and carries counter charges. It should be colorless and dispersible or dissolvable in the carrier fluid.

Figure 4 schematically shows the components of an electronic ink. The charging mechanism is based on either preferred adsorption of charged reverse micelles or acid-base interaction between the particle surface and neutral reverse micelles [10][11]. The counter-ions are stabilized by reverse micelles composed of the charge director.

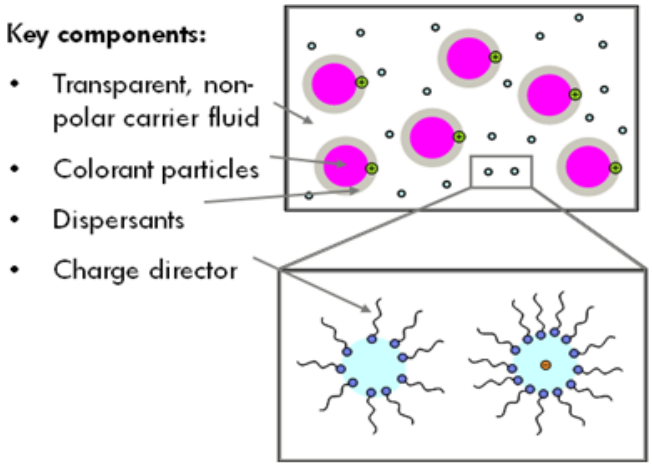

Figure 4. Schematic illustration of components of an electronic ink

In order to study structure property relationship of surfactants and their impact on device performance, a series of five polyisobutylene (PIB) succinimide surfactants were synthesized with systematic variations in the polar polyamine head and purified to separate di-substituted tails from the product (**Figure 5**). Also considered were commercially available PIB succinimide polyamine surfactant (OLOA 11000) and PIB succinic acid anhydride (OLOA 15500) from Chevron Oronite. The exact structures for the commercial products are not known. Surfactant samples were prepared to 3 wt% in isoparaffinic fluid (ExxonMobil) and sonicated for 20 minutes.

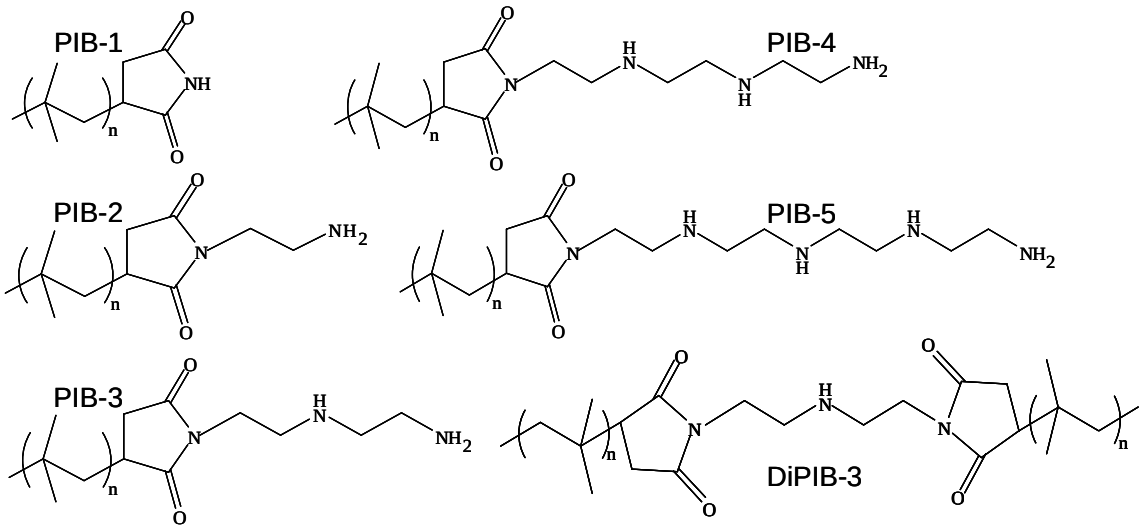

Figure 5. The structures of the synthesized surfactants. The DiPIB-3 is shown as an example the di-substituted tail by-product, which is present in each synthesis, PIB-2 through -5, separated through column chromatography.

To determine the effect of the structure of the polar head, reverse micelle shape, size, and charge were determined using small-angle light scattering (SAXS), dynamic light scattering (DLS), and transient current measurements. The SAXS measurements were conducted at the Stanford Synchrotron Radiation Lightsource. The intensity I versus scattering vector q results were modeled with NIST form factors $F(q,r)$ for a sphere and for a core-shell sphere [12]. Attempts at modeling as a cylinder or spheroid matched poorly with the data, suggesting the micelles were indeed spherical.

$$I(q) = |\Delta\rho|^2 |F(q,r)|^2 V^2(r) N$$

The electron density contrast $\Delta\rho$ was the electron density difference between the outer micelle and solvent molecules. The core-shell form factor took into account an electron density difference between the micelle core and micelle shell as well as between the micelle shell and the solvent. Micelle radius, volume, and number are represented by r, V, and N. **Figure 6** shows the fit of both models to the data. **Figure 7** shows the micelle size results.

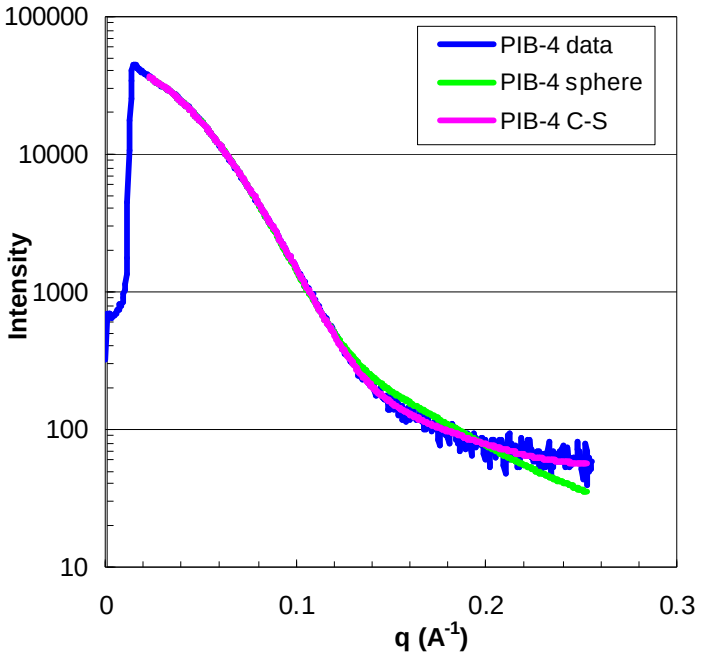

Figure 6. An example of the sphere model (green) and the core-shell model (pink) compared to the SAXS data (blue) for PIB-4. Both models fit the data well, with the core-shell model matching only slightly more closely at larger *q*.

diameter (nm)

	sphere	c+s	core
PIB-2	4.7	4.5	2.6
O11k	5.3	5.3	5.3
PIB-3	5.6	5.6	4.6
PIB-4	7.1	7.2	4.7
PIB-5	7.9	7.8	3.7
DiPIB-2	3.2	3.2	3.2
DiPIB-4	4.0	3.9	2.6
DiPIB-5	3.1	3.2	2.5

Figure 7. Micelle diameter results in nanometers for both sphere and core-shell SAXS models. Polyamines increase the diameter and double tails decrease the diameter.

The models' results indicate that SAXS is only able to measure the inner portion of the micelles. The sphere diameter is equal to the core-plus-shell diameter, not core-only diameter. Both the sphere and core-shell models fit the data similarly except at large *q*, which in inverse distance represents small length scales on the order of 1 nm. The electron density difference between the non-polar solvent and the non-polar PIB tails is low compared to the solvent and polyamine head contrast. Therefore, the SAXS is unable to resolve the tails of the micelles. In general, the results show that increasing polyamines increases the micelle core size. The OLOA 11000 most closely matches the PIB-3 size. Di-substitution of the PIB tail decreases the micelle core size, which is expected due to increased steric hindrance causing more curvature.

The DLS measurements (Malvern Zetasizer Nano ZS) gave the whole micelle size, not just the inner portion. The same trends as SAXS emerge (**Figure 8**). Increasing polyamines

increase the micelle size, OLOA 11000 falls in between PIB-2 and PIB-4, and di-substitution of the PIB tail decreases the micelle size. Interestingly, PIB-3 does not follow trend in the DLS results, perhaps due to an increased affinity for aggregation. Larger particles scatter with r^6 more intensity.

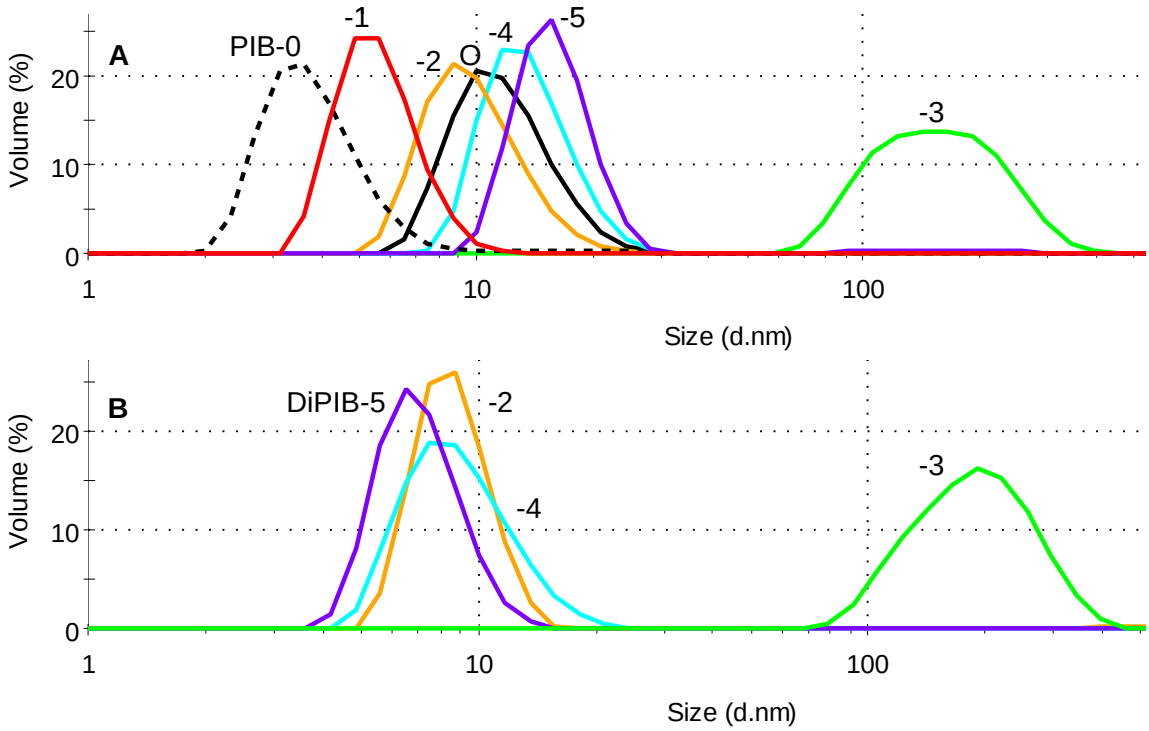

Figure 8. Volume-based size distributions in nanometers from DLS for the single-tailed surfactants in A and the double-tailed surfactants in B. Plot A also contains data for PIB succinic anhydride OLOA 15500 as "PIB-0" and OLOA 11000 as "O".

Transient current measurements applied various voltage pulses and measured recorded transient currents through LabView (National Instruments) to surfactant samples in a parallel plate cells 0.5 cm^2 × 10 μm high. In theory, during the voltage pulse, charges in the system separate to the electrodes. After the voltage is turned off, the charges re-equilibrate resulting in the transient current. The area of the transient current curve is therefore proportional to the total charge in the system [13]. **Figure 9** shows increasing polyamines increase charge concentration. The initial current is proportional to the conductivity in the system. With the conductivity and charge concentration measurements, mobility is calculated, and therefore micelle size can be determined with the Einstein relation. **Figure 10** shows a comparison of the different size measurements. The transient current method is in good agreement with DLS, which is to be expected since both are measuring the hydrodynamic radius of the whole micelle. The transient current method is less accurate for samples that have low charge, as with OLOA 15500 (PIB-0). The SAXS and DLS measurements have a consistent delta of ~6 nm for each sample, which represents the micelle tail length.

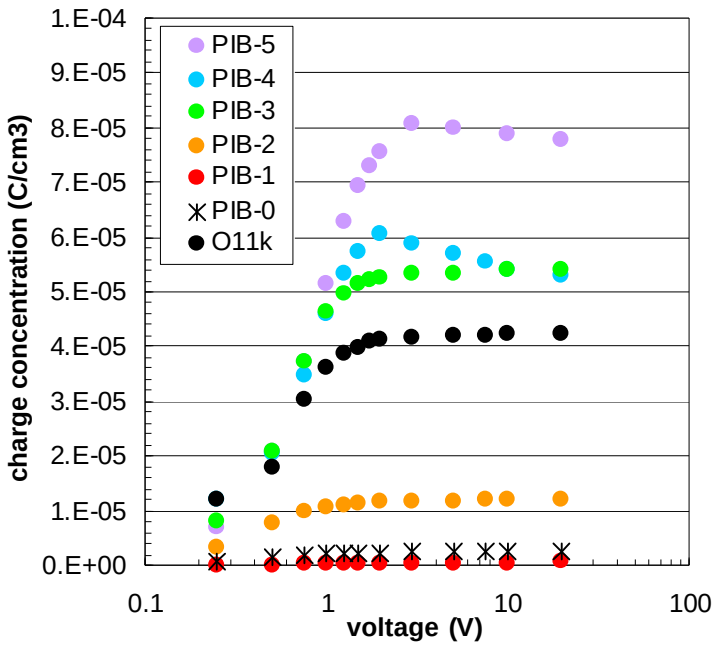

Figure 9. The charge concentration for the five synthesized surfactants as well as the PIB succinic acid anhydride OLOA 15500 as PIB-0 and OLOA 11000 as O11k.

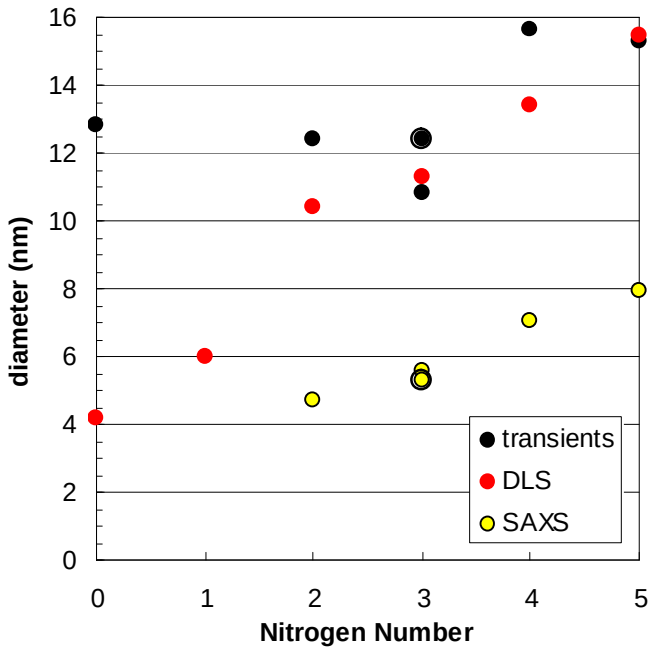

Figure 10. A comparison of the various sizing methods for each of the five synthesized surfactants as well as the PIB succinic acid anhydride OLOA 15500 at x = 0 and OLOA 11000 at x = 3 in the double outlined dots.

In order to study the impact of surfactant structures on the device performance and in turn improve performance of electronic inks through control of the charge in the system. Magenta fluids were formulated with each of the PIB surfactants and voltages were applied to the imaging fluid in test devices. Ideally, the colorant in the fluid should compact to the electrodes to enable a transparent state in the device. **Figure 11** shows how PIB-1 does not make a good Magenta dispersion while the other samples do. Polyamines of PIB-3, PIB-4 and PIB-5 show similar good compaction to the electrodes.

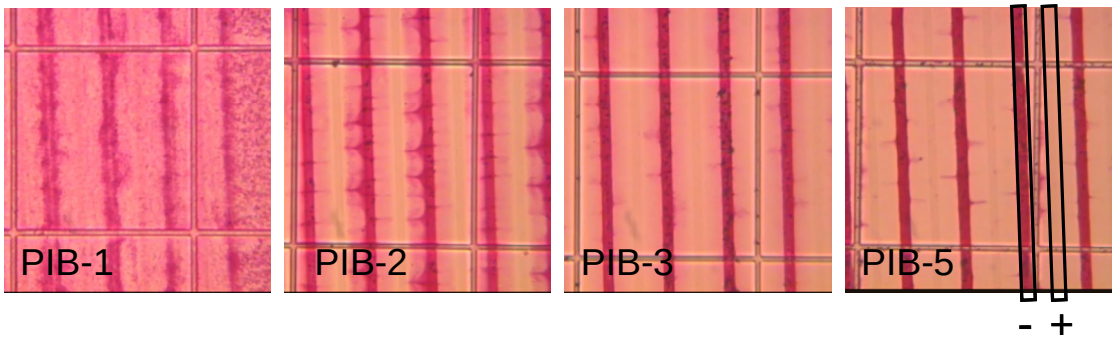

Figure 11. Test devices for Magenta fluids made with various synthesized surfactants. The right-most image shows approximately where the interdigitated electrodes are. PIB-4 is not shown since it was similar to PIB-3 and PIB-5.

Systematic variations in the polar polyamine head of a PIB surfactant showed that a terminal amine is necessary for proper charging in electrophoretic imaging fluids. The sample with just a terminal imide head (PIB-1) was the only sample that measured zero charge concentration in transient current measurements. When Magenta colorant particles were added to the PIB-1 system, they were unstable and did not compact to the test device electrodes under applied voltage. Also, various micelle sizing methods all placed OLOA 11000 at PIB-3, suggesting it has specifically a diethylene triamine head.

Roll-to-Roll (R2R) Manufacturing and Dynamic Grayscale

HP has developed new R2R processing capabilities for making fine scale circuitry on plastic substrates that is compatible with the needs of reflective displays and other devices. The processes are scalable to large web widths, and the fine features enable high density circuits and future integration with more complex passive and active elements. These R2R processes, which utilize imprint lithography and related techniques as key patterning steps, also offer significant cost advantages compared to conventional photolithographic processes [8][9]. The custom equipment set used here is capable of continuous processing of webs with widths from under 0.15 m up to 0.3 m wide. The tool set enables unit processes that include coating, imprinting, plasma treatment, electrolytic and electroless plating, and laser micro-machining.

By integrating combinations of these various processes, functional circuits are fabricated. The patterns produced can have features with minimum width dimensions of less than 5 microns, edge definition that is sub-micron, and product lengths up to 30 cm. Areas up to 150 cm^2 have been produced to date. Continuous lengths of repeating patterns are also possible, enabling very

long devices. Conductivity, flexibility and other electrical/mechanical properties that are required for a given product implementation are determined by material selection, deposition thicknesses, and process conditions.

The custom dynamic grayscale for the frontplane technology to provide full color display, grayscale addressing capability is critical. In our electrokinetic architecture, each display element that contains electrically addressable inks can be driven with direct addressing or active matrix addressing to produce continuous levels of gray. The out-of-plane switching geometry allows the control of colorants in spread and compacted states, so various grayscales can be achieved by modulating the pulse width or pulse amplitude. Providing waveforms with pulse durations faster than what the eye can resolve (< 20 ms for example) allows grayscale by controlling the specific concentration of colorant particles in the visible region of the display element. Electrokinetic frontplane technology is capable of producing greater than 3 bit gray levels. In **Figure 12**, 8 levels are demonstrated using direct driven segments along with their respective images. Continuous dynamic driving to transition from one grayscale level to another is possible without having to reset the colorant particles. **Figure 12** also illustrates this dynamic transition among various grayscale levels.

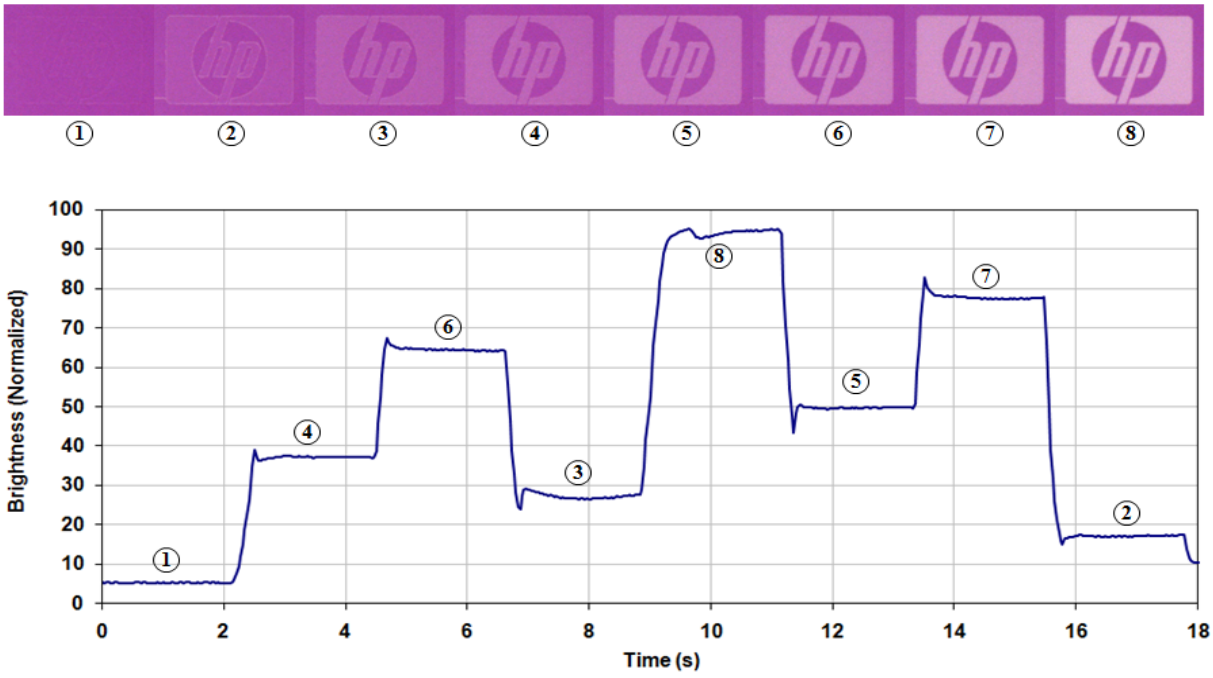

Figure 12. Dynamic driving for various levels of gray continuously addressed and held flat among 8 levels (=3bit).

Integration with Oxide TFT

Oxide TFT Backplane

For active matrix backplane, arrays of zinc indium oxide (ZIO) TFTs have been fabricated to control the voltage signal at each pixel electrode. The bottom-gate ZIO TFTs are fabricated upon a 200mm glass wafer substrate for integration with the flexible frontplane assembly; maximum backplane process temperature is 175ºC, compatible with use of either glass or

flexible plastic substrates [5]. **Figure 13** shows a schematic cross-section of the ZIO TFT backplane integrated with electrokinetic frontplane. The TFT stack is patterned using conventional photolithography (etch or lift-off); all films are deposited using sputter deposition techniques, except the HfO_x gate dielectric which is deposited using atomic layer deposition (ALD). ALD provides a means for obtaining a high-quality dielectric film at a relatively low deposition temperature of 175ºC, as compared to conventional plasma-enhanced chemical vapor deposition (PECVD) processing which can be quite challenging in this temperature range. figure demonstrates fine scale multilevel embossing capability at high yield on a flexible substrate.

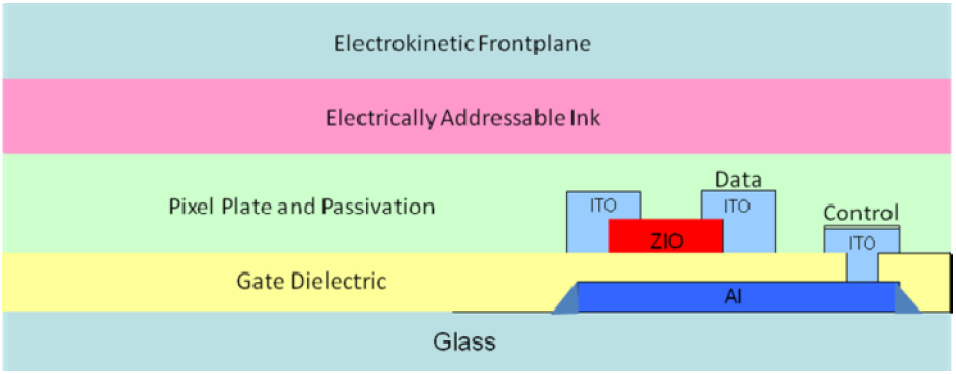

Figure 13. Schematic cross-section of integrated front and back planes.

Integration and Driving

The out-of-plane electrode geometry used in our frontplane architecture provides compatibility with active matrix backplane. The flexible frontplane media has been integrated with electrically addressable ink onto a backplane array of transparent multi-component oxide (MCO) TFTs. The plastic frontplane film is laminated onto the TFT backplane as shown from the transmission optical micrograph in **Figure 14**. To modulate the optical state of each pixel, the pixel plate electrodes are selectively activated through the TFT backplane array, while the top electrode is maintained at a fixed reference bias. Pixels are approximately 750 µm square (limited here by the dimensions of the active matrix backplane; the effective resolution of the frontplane can exceed 100 ppi). There are 1024 pixels (32 rows x 32 columns) on the proto backplane design to demonstrate the feasibility of integration and active-matrix pixelation.

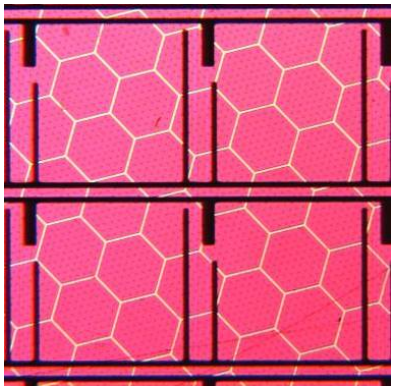

Figure 14. Transmission optical micrograph of integrated transparent TFT pixels with frontplane cells.

Figure 15 shows an integrated active-matrix electrokinetic display prototype in operation. For this device, drive voltage is limited to 10V due to the relatively thin (50 nm) HfOx gate dielectric layer (we limited HfOx gate dielectric thickness only due to practical considerations involving low ALD deposition rate). While higher voltage is preferred for optimizing electrokinetic frontplane performance, active-matrix integration and operability are clearly demonstrated. Optimization of TFT backplane to provide increased voltage drive capability is expected to provide even better optical and switching performance.

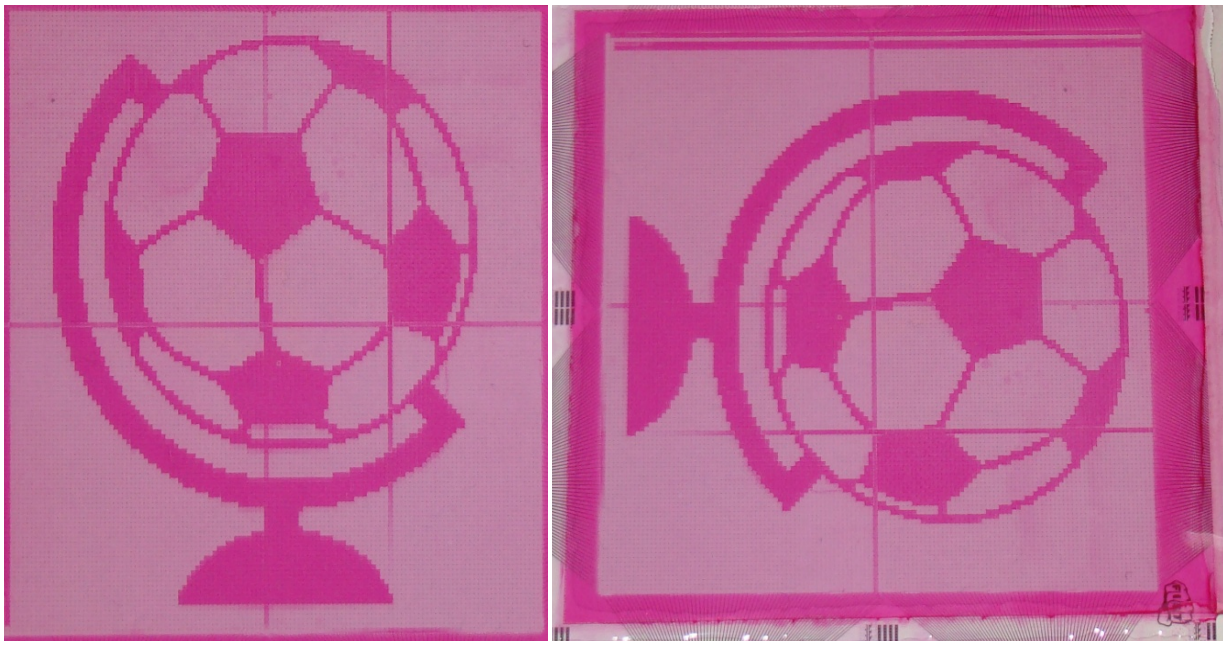

Figure 15. Integrated flexible frontplane with transparent oxide TFT backplane showing pixelation.

Integrated Print-Like Color Reflective Display Prototypes

We have successfully developed primary colorant inks and applied these novel electronic inks to segmented stacked systems. **Fig. 16a** shows each colorant layer in a segmented design, **Fig 16b, c & d** shows a three layer reflective stack of primary colorants in switching. Stacked layer design allows transflective operation enabling the use of our technology during the day with bright reflective mode or at night with front or back lighting unit.

(a) 

(b) 

(c) 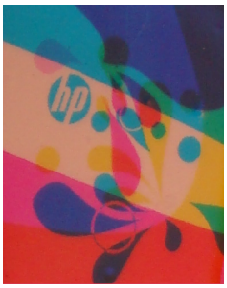
(d) 

Figure 16. (a) Individual colorant layer, (b, c, d) Color demo from segmented three layer stack with L*=23 in the fully dark state and L*=64 in the clear state with a Lambertian white reflector.

3-layer stacked devices measured with gain reflectors, which also help suppress total internal reflection loss, have 33% reflectivity or L*=65. 3-layer stacked devices with Lambertian white reflector have been measured at L*=64. Our modeling indicates white reflectance will provide L*~80 (meeting SNAP), if interfaces are index matched and the top surface is anti-reflection coated. **Fig. 17** shows the images of "world's first electronic ink based pixelated stacked color reflective display" using a three layer Cyan/Magenta/Yellow stack, each layer integrated with prototype TFT backplanes.

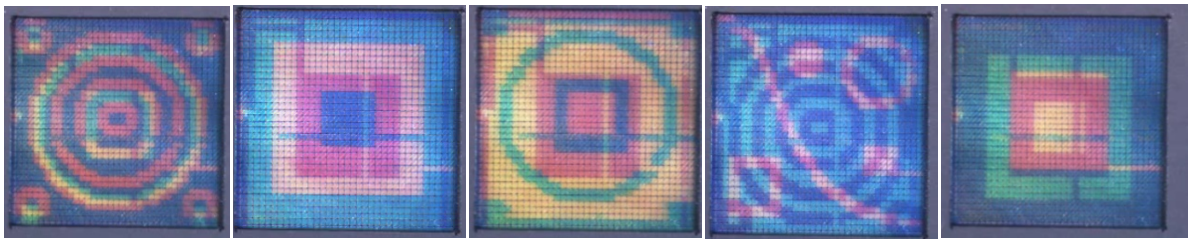

Figure 17. HP's prototype reflective display technology with print-like color.

Conclusion

A novel hybrid architecture adopting out-of-plane switching with in-plane optical effects has been demonstrated that provides a transparent state with fast switching. The results described in this paper on grayscale, pixelation, and transparency for layering moves this novel technology toward a full color reflective display demonstration. Based on optical modeling, the HP technology presented here is predicted to approach the SNAP printing standard using a system of layered colorants, enabling a level of image quality which is critical to extend the broad acceptance of full color reflective display technology. Integration of HP's R2R compatible frontplane and backplane technologies, demonstrates a scalable platform for low power, transparent, print-like media that opens up a path towards eco-friendly, bright, full color, flexible e-paper and digital signage applications. The structure property relationship of surfactants has been carried out; their impact on performance of display devices has been studied. These results have been applied to improve the performance of electronic inks. We have demonstrated 3-layer stacked segmented reflective display prototypes, as well as pixelated stacked color reflective display prototypes.

References

[1] B. Comiskey, J. D. Albert, H. Yoshizawa, and J. Jacobson, "An Electrophoretic Ink for All-Printed Reflective Electronic Displays," Nature, Vol. **394**, 253 (1998).

[2] J. Heikenfeld, P. Drzaic, J. S. Yeo, T. Koch, "A Critical Review of the Present and Future Prospects for e-Paper," J. Soc. Inf. Display, **19/2**, 129 (2011)

[3] T. Koch, D. Hill, M. Delos-Reyes, J. Mabeck, J.-S. Yeo, J. Stellbrink, D. Henze and Z.-L. Zhou, "*Late-News Paper:* Roll-to-Roll Manufacturing of Electronic Skins," SID Symposium Digest **40**, 738-741 (2009).

[4] Z. L. Zhou, J. S. Yeo, J. Mabeck, G. Combs, D. Henze and T. Koch, "Novel Digital Media

with Electronic Inks" The 31st International Congress on Imaging Science (ICIS), May 12-16, Beijing, China (2010)

[5] R. Hoffman, T. Emery, B. Yeh, T. Koch, and W. Jackson, "Zinc Indium Oxide Thin-Film Transistors for Active-Matrix Display Backplane," SID Symposium Digest **40**, 288-291 (2009).

[6] S. Swanson, M. W. Hart, and J. G. Gordon II, "High Performance Electrophoretic Displays," SID Symposium Digest **31**, 29-31 (2000).

[7] K.-M.H. Lenssen, P.J. Baesjou, F.P.M. Budzelaar, M.H.W.M. van Delden, S.J. Roosendaal, L.W.G. Stofmeel, A.R.M. Verschueren, J.J. van Glabbeek, J.T.M. Osenga and R.M. Schuurbiers, "Novel Design for Full-Color Electronic Paper," SID Symposium Digest **39**, 685-688 (2008).

[8] W. B. Jackson, C. Perolv, M. Amanza-Workman, S. Brayman, A. Chaiken, F. Jeffrey, J. Hauschildt, A. Jeans, O, Kwon, H. Luo, P. Mei, C. Taussig, "Electronics Produced by Roll-to-Roll Self-Aligned Imprint Lithography," Digest of the IEEE/LEOS Summer Topical Meetings, 125-126 (2007).

[9] J. Rudin, S. Kitson, A. Geisow, "Colour Plastic Bistable Nematic Display Fabricated by Imprint and Inkjet Technology," SID Symposium Digest **39**, 641-644 (2008).

[10] G.S. Robert, R. Sanchez, R. Kemp, T. Wood and P. Bartlett, Langmuir, **24**, 6530- 6541 (2008).

[11] I.D. Morrison, Colloids Surfaces A: Physicochem. Eng. Aspects, **71**, 1-37 (1993).

[12] S. R. Kline, Journal of Applied Crystalography, **39,** 895-900 (2006).

[13] P. Kornilovitch, and Y. Jeon. Journal of Applied Physics, **109**(6), 064509 (2011).